

D-Judge: How Far Are We? Accessing the Discrepancies Between AI-synthesized Images and Natural Images through Multimodal Guidance

Renyang Liu^{1,2} Ziyu Lyu^{*1} Wei Zhou³ See-Kiong Ng²

Abstract

In Artificial Intelligence Generated Content (AIGC), distinguishing AI-synthesized images from natural ones remains a key challenge. Despite advancements in generative models, significant discrepancies persist. To systematically investigate and quantify these discrepancies, we introduce an AI-Natural Image Discrepancy accessing benchmark (*D-Judge*) aimed at addressing the critical question: *how far are AI-generated images (AIGIs) from truly realistic images?* We construct *D-ANI*, a dataset with 5,000 natural images and over 440,000 AIGIs generated by nine models using Text-to-Image (T2I), Image-to-Image (I2I), and Text and Image-to-Image (TI2I) prompts. Our framework evaluates the discrepancy across five dimensions: naive image quality, semantic alignment, aesthetic appeal, downstream applicability, and human validation. Results reveal notable gaps, emphasizing the importance of aligning metrics with human judgment. Source code and datasets are available at <https://shorturl.at/l83W2>.

1. Introduction

With the rapid advancement of deep learning techniques, the proliferation of Artificial Intelligence Generated Content (AIGC) has garnered significant attention across various domains, such as e-commerce, gaming, medicine, animation, and autonomous driving (Li et al., 2024; Qian et al., 2024). AI-generated Images (AIGI) have been one of the mainstream forms of AIGC, and a variety of AI image generative models have been proposed to make the generated synthetic images as realistic as natural images, ranging from the earlier generative adversarial networks (GANs) (Tao et al., 2023; 2022), advanced diffusion models (DMs) (Xu

et al., 2023b; Wei et al., 2023) to the large multimodal generative model like DALL-E (Ramesh et al., 2022).

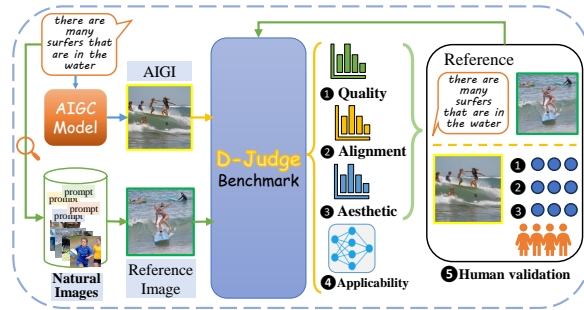


Figure 1. Toy example demonstrating the key aspects of *D-Judge*.

Despite the rapid development of AI image generative models, AI-generated images still fall short of real-world application standards due to discrepancies with realistic natural images (Li et al., 2023a). To address this, various AI-generated image quality assessment methods have emerged (Wang et al., 2023; Xu et al., 2023a; Hu et al., 2023). For instance, Wang et al. (Wang et al., 2023) introduced the AIG-CIQA2023 database and a subjective evaluation framework based on quality, authenticity, and text-image correspondence. Similarly, PKU-I2IQA (Yuan et al., 2023) developed a perception-based database for image-to-image generation using no-reference and full-reference methods. Other studies, such as Pick-a-Pic (Kirstain et al., 2023), HPS v2 (Wu et al., 2023), TIFA (Hu et al., 2023), and ImageReward (Xu et al., 2023a), focused on training unified score models for automatic AIGC image quality assessment, moving beyond traditional metrics like Inception Score (Salimans et al., 2016) and FID (Heusel et al., 2017).

Despite advancements in AIGC research, several critical issues remain unresolved. **First**, there is a lack of systematic and comprehensive studies addressing the discrepancies between AI-generated images and realistic natural images, which is crucial for enabling the practical application of AIGC images in real-world scenarios and achieving meaningful breakthroughs in the field. Most prior studies primarily focus on perceptual quality using traditional image quality metrics, text-to-image correspondence, or subjective human preferences, leaving a gap in understanding the

¹School of Cyber Security, Sun Yat-sen University ²Institute of Data Science, National University of Singapore ³Research Center of Cyberspace, Yunnan University. Correspondence to: Ziyu Lyu <lzy7@mail.sysu.edu.cn>.

broader implications of these discrepancies. **Second**, previous research predominantly considers unimodal prompts, such as T2I or I2I, while neglecting multimodal prompts like TI2I, and the datasets used are often small, typically comprising only a few thousand images, which limits their capacity for comprehensive analysis and evaluation.

To address the above challenges, we proposed an AI-Natural Image Discrepancy Evaluation Benchmark (*D-Judge*) to investigate and interpret what discrepancies still remained between AI-generated images and natural images, finally answering the important question “How far are AI generative models with respect to the visual forms of images?”. Especially, we have two important contributions with reference to the key problems. **Large Multimodal Evaluation Dataset construction:** we have curated a large multimodal evaluation dataset called *D-ANI* (Distinguishing Natural and AI-generated) dataset, with about 440,000 AIGI generated from 9 representative generative models based on both unimodal and multimodal guidance including Text-to-Image (T2I), Image-to-Image (I2I), and Text and Image-to-Image (TI2I). The data size of our DNAI dataset scales to 100x that of prior datasets. **Fine-grained Evaluation Framework,** we propose a fine-grained evaluation framework to conduct the systematic and comprehensive assessment and evaluation of DNAI, covering 5 diverse and important aspects, including naive visual feature quality, semantic alignment among multimodal generation, aesthetic appeal, downstream applicability, and the coordinated human validation. The toy example is illustrated in Figure 1. For example, given a text prompt, an image is generated using a generative model and paired with a natural reference image retrieved from the natural database. *D-Judge* then evaluates the discrepancy rate between the two images across the aforementioned dimensions.

Through our *D-ANI* dataset and fine-grained evaluation framework *D-Judge*, we conduct extensive benchmark analysis and evaluation and conclude key insights to answer the discrepancy questions:

- **Significant discrepancies in key Areas:** *AIGIs exhibit substantial discrepancies from natural images in terms of quantitative measures from all aspects, up to 40%, 33.57%, 27.66%, and 96.95% in frame-level image quality, semantic alignment, aesthetic appeal, and downstream applicability, respectively.*
- **Multimodal Alignment:** Different prompted generations might have different semantic alignment discrepancies compared to natural ones. *Generated images prompted with texts including both T2I and TI2I demonstrated less semantic discrepancy than I2I.*
- **Downstream Task Applicability:** *Significant differences in usability between AI-generated and natural images are observed in downstream tasks, particularly in*

fine-grained object recognition and VQA, with discrepancy rates reaching as high as 94.29% and 96.95%, respectively. This underscores the need for further advancements in generative models to enhance their practical applicability in real-world scenarios.

- **Human Evaluation vs. Quantitative Metrics:** *Human evaluation results reveal larger discrepancies compared with quantitative ones. It validates the necessity of incorporating human evaluation for coordination.*

2. Related Work

Natural Image Evaluation: Over the past decades, numerous image quality assessment methods have been developed to evaluate natural images (N. et al., 2015). These methods have focused on various visual features and properties, such as perceptual appearance (Zhang et al., 2018), naturalness (Ma et al., 2018), and aesthetics (Esfandarani & Milanfar, 2018). For instance, BRISQUE evaluates natural image quality by analyzing spatial domain features, while PIQE assesses perceptual quality through block-based image segmentation, both serving as effective no-reference metrics. Other notable measures include FID and Inception Scores, which assess the quality and diversity of generated images, and SSIM (Wang et al., 2004) and PSNR, which quantify structural similarity and pixel-level accuracy. Beyond quantitative measures, human evaluations have also been leveraged to estimate natural image quality. For example, NIMA (Esfandarani & Milanfar, 2018), proposed by Talebi and Milanfar, uses a deep CNN trained on human-rated images to predict aesthetic quality. Similarly, Wong et al. introduced the AVA dataset, which facilitates aesthetic assessment based on human preferences (Murray et al., 2012).

AI-generated Image Evaluation: Recently, AI-generated content (AIGC) has seen significant advancements with the rise of generative models. Several methods and benchmarks have been introduced to evaluate AI-generated images (Zhang et al., 2023; Hu et al., 2023). These methods primarily focus on three aspects: perceptual quality, text-image correspondence, and aesthetics (Xu et al., 2023a; Wang et al., 2023), often training unified models to assess the overall quality of AI-generated images. For example, ImageReward (Xu et al., 2023a) presents a framework for aligning image generation with human preferences, AGIQA-3k (Li et al., 2023a) offers a comprehensive benchmark for assessing AI-generated image quality, and QBench (Wu et al., 2024a) evaluates content quality across multiple dimensions.

Despite advancements, little research has delved into the fine-grained differences between AI-generated and natural images, and existing datasets are often too small for comprehensive evaluation. To address these gaps, we propose

D-Judge as AI-Natural image difference Assessment Benchmark, featuring a large Distinguishing AI-Natural Image Dataset and a systematic, fine-grained evaluation framework to thoroughly explore these differences.

3. D-Judge

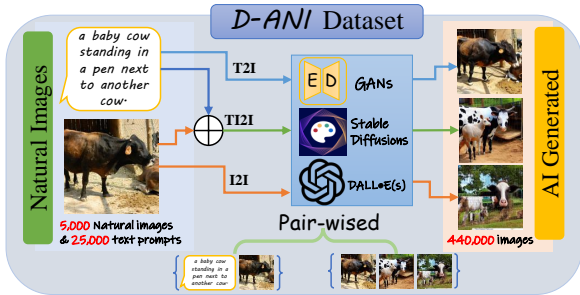


Figure 2. The *D-ANI* dataset of *D-Judge*, guided by three types of prompts. Each generated image is paired with both the corresponding text and image from the naturally collected dataset (e.g., COCO).

To tackle the challenges of current AI-generated image evaluation, we construct an AI-Natural Image Discrepancy evaluation benchmark (*D-Judge*) to assess the potential discrepancies between AI-generated images and natural images and answer how far AIGIs are from Natural Images. Firstly, a Distinguishing AI-Natural Image (*D-ANI*) Dataset is constructed, in which we collect AI-generated images from diverse generative models for real natural images in MS COCO dataset (Lin et al., 2014) based on three types of guidance prompts, e.g., text-only, image-only and text-image prompts, as shown in Figure 2; Then, we devise a systematic and comprehensive evaluation framework as Figure 3 illustrated to measure and evaluate the potential differences between AI-generated images and real natural images from five aspects including naive image quality, semantic alignment, aesthetic appeal, downstream applicability, and the coordinated human assessment. In the following parts, we introduce the *D-ANI* Dataset and the evaluation framework in detail.

3.1. Distinguishing AI-Natural Image Dataset

We construct the Distinguished Natural and AI-generated Image Dataset based on the classical natural image dataset MS COCO dataset. We select 5,000 images covering diverse captions from the MS COCO dataset and collect a total of 25,000 text-image pairs by pairing each image with five different pieces of text descriptions. The 25,000 text-image pairs are seen as the **referenced natural image set**.

For each text-image sample in the referenced natural image set, we collect AI-generated images from 9 representative generative models, guided by three types of prompts, includ-

Table 1. Comparison of *D-ANI* dataset and Counterparts.

Dataset	Model	Text	Image	Text vs. Image	AIGI
AGIQA-1K	2	1,080	-	-	1,080
AGIQA-3K	6	300	-	-	2,982
AIGCIQA2023	6	100	-	-	2,400
PKU-I2IQA	2	200	200	-	1,600
<i>D-ANI</i> (Ours)	9	25,000	5,000	25,000	445,000

ing text-only prompts, image-only prompts, and text-image prompts. The 9 representative generative models are from diverse generative models ranging from the earlier generative adversarial networks (GANs) (e.g. GALIP (Tao et al., 2023), DF-GAN (Tao et al., 2022)) to the recent diffusion models (DMs) like Stable Diffusion v1.4 (SD14), v1.5 (SD15), v2.1 (SD21), XL (SDxl) (Rombach et al., 2022), Versatile-Diffusion (VD) (Xu et al., 2023b), OpenAI DALL-E 2 (D-E 2) (Ramesh et al., 2022) and DALL-E 3 (D-E 3) (OpenAI, 2024). The referenced natural images and the generated images comprise our distinguishing AI-Natural image dataset. More details about data construction and collection are presented in Appendix Sec. B.

Table 1 shows the statistics and properties of our *D-ANI* Dataset compared with the existing evaluation dataset. Our *D-ANI* Dataset has a total of 440,000 AI-generated images from 9 representative generated models. For details, please refer to Appendix Sec. B. Compared with state-of-the-art evaluation datasets, our *D-ANI* Dataset has convincing contributions:

- *D-ANI* Dataset is the most extensive dataset for AI-generated image evaluation, and the **data size scales to 100x**.
- *D-ANI* Dataset is guided by both **unimodal prompts and multi-modal prompts (text-image)**. Prior datasets barely considered text prompts.
- **Comprehensive and Diverse generative models are exploited**, ranging from the earlier GAN models, the recent popular diffusion models, and the influential large commercial generative model DALL-E 2 and DALL-E 3 issued by OpenAI.

Our large and comprehensive dataset works as the foundation of the assessment benchmark and enables thorough evaluation and analysis of the differences between AI-generated images and realistic natural images.

3.2. *D-Judge* Framework

On top of the *D-ANI* dataset, we construct the fine-grained *D-Judge* to systematically measure and interpret the differences between AI-generated images and realistic natural images from five key different aspects as following aspects.

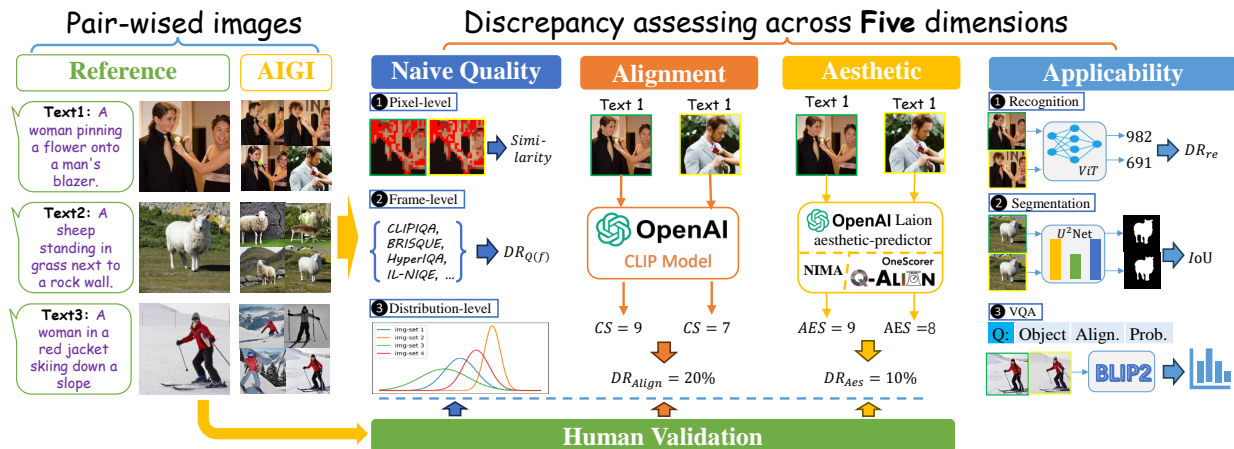


Figure 3. The framework of *D-Judge* evaluates the **Discrepancy Rate** (DR) between AI-generated images and natural reference images across **five** dimensions: ❶ *Naive Quality*, ❷ *Alignment*, ❸ *Aesthetic*, and ❹ *Applicability*, complemented by ❺ **human validation**. The images with **green borders** represent reference natural images, while those with **yellow borders** are AI-generated counterparts. This comprehensive evaluation integrates pixel-level, frame-level, and distribution-level quality checks, alongside advanced tools like *OpenAI CLIP*, *OpenAI Laion Aesthetic Evaluator*, *Qalign*, *ViT*, *U²Net*, and *BLIP2* to robustly assess the gap between the two image types. Where CS means CLIP Score for the text and given images, and AES means Aesthetic score.

1. Naive Image Quality Discrepancy: We leverage traditional image quality assessment methods for natural images to measure the AI-Natural image differences. In order to perform fine-grained analysis and exploration, we estimate the AI-Natural image differences from three levels by considering the inherent properties of image-style content, ranging from the **pixel-level visual features**, **frame-level visual features** to the **holistic content distribution**.

- First, we use the full-referenced **pixel-level similarity measures** like SSIM, LPIPS, and DISTS to compute the **visual similarities** between the paired AI-generated image and natural image and use these calculated values to quantify the AI-Natural image differences from the low-level visual view.
- Second, we use non-referenced **frame-level visual features** to qualify the perceptual quality of images and compute the frame-level visual quality difference rates between AI-generated images and natural images from the high-level visual view. The exploited frame-level visual features include PIQE (N. et al., 2015), IL-NIQE (Zhang et al., 2015), MUSIQ (Ke et al., 2021), DBCNN (Zhang et al., 2020), LIQE (Ma et al., 2018), Inception Score (Salimans et al., 2016), CLIPQA (Radford et al., 2021b), TReS (Gu et al., 2015), HyperIQA (Su et al., 2020), UNIQUE (Zhang et al., 2021), BRISQUE, NIQE (Mittal et al., 2013), NRQM (Ma et al., 2018), etc. The Discrepancy Rate (DR) of these metrics provides insights into frame-level visual quality differences.
- Third, we investigate the full-reference **visual content distribution** to capture the holistic differences between AI-generated images and natural images by computing

the FID, CLIP-FID, and Inception Score of the AI-generated image set and the referenced natural image set. The results of these set-level measures can reflect the difference between AIGIs and natural ones from an integral perspective.

Based on the different levels of image quality measures, our framework can assess and measure the fine-grained AI-Natural images differences with Full-reference and Non-reference angles, covering both low-level and high-level. More details about the utilized traditional image quality assessment measures are described in Appendix Sec. C.

2. Semantic Alignment Discrepancy: Generative models require the referenced prompts as semantic guidance to generate images. Therefore, semantic alignment can be an important quality indicator of the AIGIs. We use the widely used CLIP model (Radford et al., 2021a) to calculate the difference rates of Clip Scores, DR_{CS} to represent alignment discrepancies between AIGIs and natural images, and provide a fine-grained analysis with respect to both unimodal and multimodal guidance.

3. Aesthetic Appeal Discrepancy: Aesthetic Appeal is to estimate the visual appeal and artistic quality of images, reflecting the visual attractiveness and artistic quality of images. We utilize the classical aesthetic measures NIMA (Esfandarani & Milanfar, 2018), LAION-AES (Schuhmann et al., 2022a), and QAlign (Wu et al., 2024b) as the quantitative metrics and compare the difference rates of aesthetic scores DR_{aes} for the paired AI-generated and natural images.

4. Downstream Applicability Discrepancy: This aspect is devised to investigate the practical utility of AI-generated images in downstream tasks and evaluate whether AI-generated images can have different practical utilities with realistic natural images in downstream application tasks. We mainly focus on three common downstream tasks, e.g., image recognition, object segmentation and Multimodal Visual Question Answering (VQA). For the image recognition task, we evaluate the Difference recognition rates (DR_{re}) between AI-generated images and natural images when using a pre-trained image recognizer like ResNet-152 (He et al., 2016) model. For the object segmentation, we use the Intersection over Union (IoU) (Everingham et al., 2010) as quantitative measures and investigate the segmentation discrepancy for AI-generated images with U²Net (Qin et al., 2020). For VQA, we design three types of questions: ‘object’ (identifying objects in the image), ‘alignment’ (determining if the image aligns with a textual description, returning ‘yes’ or ‘no’), and ‘similarity probability’ (calculating the alignment probability between text and image). Using BLIP2 (Li et al., 2023b), we evaluate the *Difference Rate (DR)* between AI-generated images and reference natural images for each question type.

5. Human Validation: We involve human assessments to coordinate the above evaluation aspects. We develop the human assessment interface to demonstrate AI-generated images with the referenced natural images and text descriptions and collect human ratings (on a scale from 1 to 5) alongside the following three aspects: naive image quality, semantic alignment, and Aesthetic Appeal as human assessments. Human participants are provided with example images before the evaluation to understand high and low scores without being given specific numerical values, ensuring unbiased and informed ratings. Detailed information about human assessment procedures is provided in Appendix Sec. D.3.

Through the integration of diverse and comprehensive evaluated dimensions, our *D-Judge* offers a systematic assessment solution to investigate and interpret the differences that still remain between AI-generated images and natural images.

4. Evaluation

With respect to the 5 different aspects, we conducted benchmark experiments and performed experimental evaluation alongside the following research questions.

RQ1: What are the fine-grained naive image quality discrepancies between AIGIs and natural images?

- **RQ1.a:** What discrepancies between I2I-guided AIGIs and their natural counterparts can be interpreted via the

pixel-level quality measures?

- **RQ1.b:** What discrepancies between multimodal-guided AIGIs and their natural counterparts can be revealed via the frame-level metrics?
- **RQ1.c:** How do the structural visual content distributions differ between AIGIs and natural images?

RQ2: How significant are the discrepancies in the semantic alignment of the given text with natural images and AIGIs in different types of guidance?

RQ3: What are the discrepancies in aesthetic appeal between AIGIs and natural images?

RQ4: How do AIGIs differ from natural images in downstream task applicability?

RQ5: Are human assessment results consistent with quantitative measures? What are the discrepancies revealed from human evaluation?

4.1. Experimental Setting

We use the described quantitative evaluation metrics, which can be divided into Full-reference and No-reference, to present the *DR* for involved assessment dimensions (more details of all metrics are presented in Appendix Sec. C).

Full-reference metrics: For full-reference metrics, which are used for pixel-level image quality, visual content distribution, and downstream object segmentation task, i.e., IoU, we directly report the calculated value to reflect the difference cause it already can present the discrepancy.

No-reference metrics We calculate *Difference Rate (DR)* for each quantitative metric in non-reference scenarios, by subtracting the value of each AI-generated image from its corresponding natural reference image and then averaging these difference rates, defined as follows:

$$DR = \frac{1}{n} \sum_{i=1}^n \frac{|(M(\mathbf{X}_i) - m_{\min}) - (M(\mathbf{N}_i) - m_{\min})|}{m_{\max} - m_{\min}} \quad (1)$$

where n is the number of images, M represents the metric, \mathbf{X} denotes the generated images, and \mathbf{N} refers to the referenced natural images. Additionally, m_{\min} and m_{\max} represent the minimum and maximum values across all images, respectively, especially when the value range of the corresponding metric is undefined.

4.2. RQ1: Naive Quality Results

To evaluate the image quality of AI-generated images versus natural images, we conducted a comprehensive analysis using a variety of metrics that assess the discrepancies between AIGIs and natural images across pixel-level similarity, frame-level quality and visual content distribution. ***Our find-***

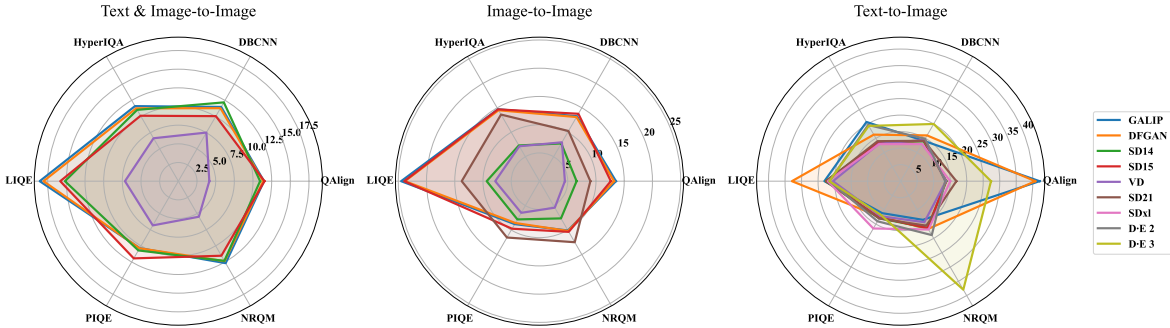


Figure 4. We evaluate nine image-generating models from 6 aspects. The numerical values in the radar chart represent the mean difference rate of each model.

Table 2. Full-reference Evaluation Results (I2I).

	SD14	SD15	VD	SD21	SDx1	D-E 2
SSIM \uparrow	0.35	0.35	0.46	0.43	0.70	0.37
PSNR \uparrow	13.72	13.71	16.41	15.86	23.11	12.29
VIF \uparrow	0.02	0.02	0.05	0.04	0.18	0.03
VSI \uparrow	0.84	0.84	0.89	0.87	0.96	0.83
FSIM \uparrow	0.61	0.61	0.71	0.66	0.86	0.60
LPIPS \downarrow	0.60	0.60	0.39	0.52	0.19	0.61
DISTS \downarrow	0.27	0.27	0.17	0.23	0.10	0.24
MAD \downarrow	212.91	213.09	197.92	203.89	144.92	217.12

ings reveal substantial discrepancies between AIGIs and natural images across these dimensions.

4.2.1. RQ1.A PIXEL-LEVEL

We evaluated the visual similarity between AI-generated and natural images using structural metrics like SSIM, LPIPS, DISTS, PSNR, etc. The mean similarity values of these metrics, as shown in Table 2, indicate that **AI-generated images exhibit significantly lower similarity to natural counterparts**. AI-generated images show a 30% to 65% reduction in SSIM, highlighting a major loss in structural fidelity. LPIPS and DISTS further reveal notable perceptual dissimilarities, with LPIPS scores ranging from 0.19 to 0.61. Additionally, PSNR values between 12.29 and 23.11 suggest that AI-generated images have higher noise levels, reducing their overall visual similarity.

4.2.2. RQ1.B FRAME-LEVEL

We assessed the frame-level discrepancies of AI-generated and natural images using a suite of metrics, including DBCNN, HyperQA, LIQE, PIQE, NRQM and QAlign. Figure 4 uses radar figures to visualize the mean difference rates from the six metrics, and indicates that **there are significant quality differences between AI-generated and natural images at the frame level**. These deviations are typically around 10%, irrespective of the guidance prompt used, with some instances showing quality differences as high as 40%. This underscores the considerable gaps between

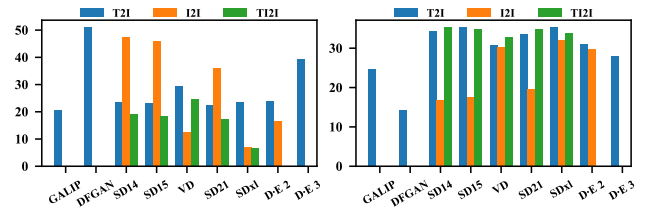


Figure 5. The FID (left, \downarrow) and Inception Score (right, \uparrow) of AI-generated images from different source models and guidance.

AIGIs and natural images in terms of global image quality. Moreover, the results of NRQM reveal that **AI-generated images significantly differ from natural images in terms of naturalness**. Specifically, AI-generated images show notable deviations from natural images in visual realism and adherence to natural scene statistics. The NRQM difference rates range from 5% to 32%, with images generated by D-E 3 exhibiting particularly high rates, underscoring the challenges AI-generated images encounter in replicating the inherent naturalness of real-world scenes. More detailed results with more metrics are presented in Appendix Sec. D.1 Figure 12.

4.2.3. RQ1.C VISUAL CONTENT DISTRIBUTION

We present the FID and Inception Score results, presented in Figure 5, suggesting that AI-generated images often exhibit relatively higher FID scores (up to 50) and lower Inception Scores (low to 14). **This finding indicates that current generative models, particularly GAN-based models and earlier versions of Stable Diffusion, struggle to produce high-quality images as naturally collected images consistently**. Notably, these models tend to generate better images when a reference image is provided (TI2I), as it has more detailed guidance.

In conclusion, **our evaluation of image quality across pixel-level, frame-level, and content distribution-level reveals significant disparities between AI-generated and natural images**. These differences highlight the current limitations of AIGC technologies in matching the visual

Table 3. The results of DR_{CS} (%).

	GALIP	DFGAN	SD14	SD15	VD	SD21	SDx1	D-E 2	D-E 3
T2I	12.16	16.11	10.67	10.53	9.71	10.90	11.59	10.93	10.19
I2I	-	-	33.43	33.57	4.89	24.04	3.56	5.53	-
TI2I	-	-	9.90	9.73	8.22	9.20	3.57	-	-

quality and realism of natural images.

4.3. RQ2: Alignment Results

We calculate the difference rate of CLIP Scores (DR_{CS}) to assess how well the AIGIs align with natural ones in terms of semantic alignment across different guidance types: Text-to-Image (T2I), Image-to-Image (I2I), and Text-and-Image-to-Image (TI2I). And we find that *AIGIs often struggle to maintain semantic alignment as natural ones, especially the image-only reference provided*. The results, shown in Table 3, indicate that the DR_{CS} range from 4.02% to 36.69%. We also find that *even if the AIGIs can get a higher CS sometimes, especially with text and image-guided, they are looking stranger to humans*. This suggests that current AIGC models often struggle to maintain high fidelity to the provided references, leading to variations that may impact the intended alignment. Our findings underscore the challenges that these models face in consistently generating content to accurately reflect the specified input conditions, highlighting both their strengths and limitations in real-world applications.

4.4. RQ3: Aesthetic Appeal

We assessed the aesthetic appeal of AI-generated and natural images using NIMA and LAION-AES metrics and found that *AI-generated images generally fall short of natural images in terms of aesthetic quality*. Figure 6 presents the aesthetic difference rate (DR_{aes}) results, which reveal that AI-generated images have noteworthy discrepancies compared to natural ones, with DR_{aes} ranging from 3.51% to 27.66%. These findings indicate that while AI models can produce visually appealing images, *AIGIs’ often lack the nuanced artistic quality and emotional impact that are characteristic of natural images*.

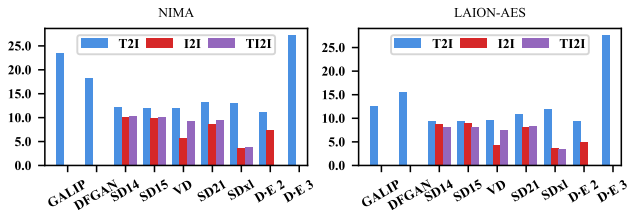


Figure 6. The DR_{aes} between AIGIs and natural ones.

4.5. RQ4: Applicability Results

When evaluating the applicability of AI-generated images, we focused on three crucial downstream tasks: image recognition, semantic segmentation and VQA. Our findings indicate *significant discrepancies between the performance of AIGC images and natural images in these tasks*.

Image Recognition: We measured the classification *Difference Rate (DR)* (%) to identify the differences in predicted labels between AIGC images and their natural counterparts. The results in Table 8 showed a substantial gap, with the DR ranging from 27.46% to 94.29%, indicating that the generated images can’t accurately present the object as expected.

Semantic Segmentation: We evaluated the performance using the Intersection over Union (IoU) metric and show the discrepancy results in Table 9. The *IoU* values (higher is better) for AIGC images varied between 0.33 and 0.82, indicating a wide range of segmentation between AIGC images and their natural counterparts.

Visual Question Answering: Further, we apply these AI-generated image to the VQA task by BLIP-2 (Li et al., 2023b) involved three different types of questions: Object, Alignment (Align), and similarity probability (Prob.). Table 4 summarizes the discrepancies (%) between natural and AI-generated images across various questions. For Object, the highest discrepancies occurred in the I2I setting, with SD14 and SD15 reaching 96.41% and 96.95%, respectively, while T2I discrepancies ranged from 64.07% (DALL-E 3) to 88.43% (DFGAN). Align questions showed lower discrepancies, with T2I values ranging from 8.55% (DFGAN) to 21.18% (DALL-E 3) and I2I values from 7.87% (VD) to 10.07% (SD15). For similarity probability (Prob.), T2I discrepancies varied between 37.31% (DALL-E 2) and 62.69% (DFGAN), while I2I results ranged from 32.81% (DALL-E) to 61.56% (SD15).

Overall, our findings highlight significant limitations of AI-generated images in tasks such as image recognition, semantic segmentation, and visual question answering (VQA). While AI-generated images perform comparably to natural images in simpler tasks, such as binary text-image alignment (e.g., responding with “yes” or “no”), they fall short in more complex scenarios, including accurately estimating text-image alignment probabilities, identifying specific objects, and segmenting object areas. These shortcomings limit their broader applicability in diverse downstream tasks compared to natural images. Our results underscore the need for continued research and development to improve the reliability and accuracy of AIGC models, enabling their effective deployment in real-world applications.

Table 4. The Difference Rate (DR) of VQA tasks.

		GALIP	DFGAN	SD14	SD15	VD	SD21	SDxl	D-E 2	D-E 3
Object	T2I	73.34	88.43	68.72	68.63	74.21	68.34	66.93	57.85	64.07
	I2I	-	-	96.41	96.95	50.43	91.14	51.65	46.29	-
	TI2I	-	-	67.22	66.65	66.29	67.22	49.20	-	-
Align	T2I	10.57	8.55	14.02	15.79	12.32	13.02	13.00	12.99	21.18
	I2I	-	-	9.71	9.53	7.87	10.07	8.01	8.93	-
	TI2I	-	-	13.31	12.70	10.03	10.99	8.46	-	-
Prob.	T2I	53.13	62.69	53.07	54.21	50.57	54.95	57.09	37.31	49.22
	I2I	-	-	61.05	61.56	39.57	58.67	43.64	32.81	-
	TI2I	-	-	50.96	50.34	45.93	49.97	41.48	-	-

4.6. Human Validation

To rigorously assess the differences between AI-Natural images and to evaluate the effectiveness of existing metrics in measuring AIGC image quality, we conducted human evaluations focusing on three key aspects: Image Quality, Alignment, and Aesthetic Appeal.

- **Image Quality:** Participants assessed the overall quality of the images, considering factors such as clarity, detail, and the presence of artifacts.
- **Alignment:** This aspect measured how well the generated images matched the given prompts.
- **Aesthetic:** The aesthetic appeal of the images was rated based on visual attractiveness, composition, and overall artistic quality.

We excluded results for Applicability since this dimension inherently involves human-generated ground truth labels. Participants rated images on a scale from 1 (poor) to 5 (excellent). Our human evaluation results are shown in Table 5 and Figure 7 reveal *significant discrepancies between AI-generated images and natural images across all three assessed aspects: quality, alignment, and aesthetic appeal*. AIGC images consistently received lower scores across all three dimensions; AI-generated images generally received lower scores, often between 2 and 3, compared to natural images. This emphasizes the need for further advancements to narrow these gaps. These findings underscore the importance of continued research and development in AI image generation to bring AIGC images closer to the standards of natural images.

Moreover, the result in Figure 7 from human validation indicates that *traditional quantitative metrics often fail to align with human preferences, suggesting that they are not fully compatible with assessing AIGC images*. This highlights the necessity for developing new measures tailored specifically to the unique characteristics of AI-generated content.

Table 5. Human score results across three aspects.

	SD21		SDxl			VD			D-E 2	
	T2I	I2I	TI2I	T2I	I2I	TI2I	T2I	I2I	TI2I	T2I
Quality	3.54	3.68	2.88	3.44	2.40	4.39	4.11	3.49	3.31	4.37
Alignment	3.45	3.43	2.48	3.16	2.44	4.47	4.22	3.59	3.40	4.50
Aesthetic	3.38	3.55	2.70	3.21	2.35	4.29	3.96	3.32	3.19	4.28

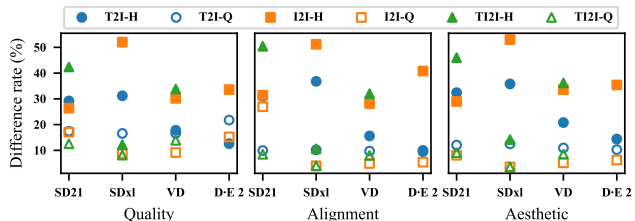


Figure 7. The difference rate provided by human & quantitative statistics, where ‘H’ represents human and ‘Q’ represents quantitative.

4.7. Discrepancies Across Categories

To analyze the differences between AI-generated and natural images across various categories, we evaluated the discrepancy of AIGI from eight categories (‘person’, ‘animal’, ‘indoor’, ‘outdoor’, ‘vehicle’, ‘food’, ‘sports’, ‘accessory’) across three key aspects: ① **Naive Quality**, including pixel-level similarity (SSIM), frame-level quality (CLIPQA), and content distribution (FID, CLIP-FID, and Inception Score); ② **Alignment**, measured by CLIP Score; and ③ **Aesthetic Quality**, assessed by LAION-AES. The results in Figure 8 reveal substantial variability across different categories, even for the AIGI from the same model (please refer to Appendix Sec. D.2, Figures 16 and 17 for integrated details). This could be attributed to the significant imbalance in the distribution of training data across these categories (Schuhmann et al., 2022b; Aghajanyan et al., 2023).

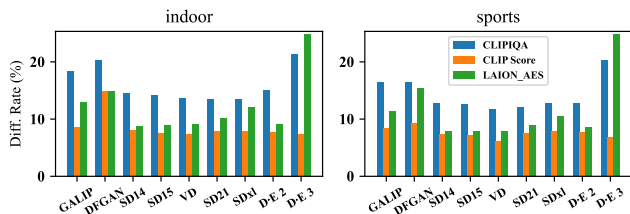


Figure 8. The difference rate on food and sport subcategories across quality, alignment, and aesthetic.

5. Conclusion and Discussion

In this paper, we develop a systematic and comprehensive *D-Judge* to evaluate the discrepancies between AI-Natural images using the constructed *D-ANI* dataset. Our findings reveal significant disparities in naive image quality, semantic

alignment, aesthetics, and downstream task applicability, especially in the low-level and content distribution-level image quality and fine-grained downstream tasks, like object recognition and object VAQ. While AIGC models have achieved impressive innovations, AIGIs still lag behind natural images in these critical areas. Besides, human evaluations also reveal lower scores for AIGC in terms of visual quality, semantic alignment, and aesthetics, emphasizing the gaps between AIGIs and natural images. Finally, the poor utility of AIGIs in downstream tasks indicates practical application challenges for AIGC.

This study also has limitations, including reliance on specific quantitative metrics and models available at the time. Future studies should incorporate more generative models, larger datasets, and sophisticated metrics to capture further discrepancies. Addressing these limitations and improving models will help reduce the perceptual gaps between AIGC images and natural images, facilitating better integration into real-world applications.

Impact Statement

This paper presents work whose goal is to advance the field of Machine Learning. There are many potential societal consequences of our work, none which we feel must be specifically highlighted here.

References

- Aghajanyan, A., Yu, L., Conneau, A., Hsu, W., Hambarzumyan, K., Zhang, S., Roller, S., Goyal, N., Levy, O., and Zettlemoyer, L. Scaling laws for generative mixed-modal language models. In *ICML*, pp. 265–279, 2023.
- Ding, K., Ma, K., Wang, S., and Simoncelli, E. P. Image quality assessment: Unifying structure and texture similarity. *IEEE Trans. Pattern Anal. Mach. Intell.*, 44(5): 2567–2581, 2022.
- Esfandarani, H. T. and Milanfar, P. NIMA: neural image assessment. *IEEE Trans. Image Process.*, 27(8):3998–4011, 2018.
- Everingham, M., Gool, L. V., Williams, C. K. I., Winn, J. M., and Zisserman, A. The pascal visual object classes (VOC) challenge. *Int. J. Comput. Vis.*, 88(2):303–338, 2010.
- Gu, K., Zhai, G., Yang, X., and Zhang, W. Using free energy principle for blind image quality assessment. *IEEE Trans. Multimed.*, 17(1):50–63, 2015.
- He, K., Zhang, X., Ren, S., and Sun, J. Deep residual learning for image recognition. In *CVPR*, pp. 770–778, 2016.
- Heusel, M., Ramsauer, H., Unterthiner, T., Nessler, B., and Hochreiter, S. Gans trained by a two time-scale update rule converge to a local nash equilibrium. In *NeurIPS*, pp. 6626–6637, 2017.
- Hu, Y., Liu, B., Kasai, J., Wang, Y., Ostendorf, M., Krishna, R., and Smith, N. A. TIFA: accurate and interpretable text-to-image faithfulness evaluation with question answering. In *ICCV*, pp. 20349–20360, 2023.
- Kang, L., Ye, P., Li, Y., and Doermann, D. S. Convolutional neural networks for no-reference image quality assessment. In *CVPR*, pp. 1733–1740, 2014.
- Ke, J., Wang, Q., Wang, Y., Milanfar, P., and Yang, F. MUSIQ: multi-scale image quality transformer. In *ICCV*, pp. 5128–5137, 2021.
- Kirstain, Y., Polyak, A., Singer, U., Matiana, S., Penna, J., and Levy, O. Pick-a-pic: An open dataset of user preferences for text-to-image generation. In *NeurIPS*, 2023.
- Kynkäänniemi, T., Karras, T., Aittala, M., Aila, T., and Lehtinen, J. The role of imagenet classes in fréchet inception distance. In *ICLR*, 2023.
- Larson, E. C. and Chandler, D. M. Most apparent distortion: full-reference image quality assessment and the role of strategy. *J. Electronic Imaging*, 19(1):011006, 2010.
- Li, C., Zhang, Z., Wu, H., Sun, W., Min, X., Liu, X., Zhai, G., and Lin, W. AGIQA-3K: an open database for ai-generated image quality assessment. *CoRR*, 2023a.
- Li, J., Li, D., Savarese, S., and Hoi, S. C. H. BLIP-2: bootstrapping language-image pre-training with frozen image encoders and large language models. In *ICML*, pp. 19730–19742, 2023b.
- Li, M., Cai, T., Cao, J., Zhang, Q., Cai, H., Bai, J., Jia, Y., Li, K., and Han, S. Distrifusion: Distributed parallel inference for high-resolution diffusion models. In *CVPR*, pp. 7183–7193, 2024.
- Lin, T., Maire, M., Belongie, S. J., Hays, J., Perona, P., Ramanan, D., Dollár, P., and Zitnick, C. L. Microsoft COCO: common objects in context. In *ECCV*, volume 8693, pp. 740–755, 2014.
- Ma, K., Liu, W., Zhang, K., Duanmu, Z., Wang, Z., and Zuo, W. End-to-end blind image quality assessment using deep neural networks. *IEEE Trans. Image Process.*, 27(3):1202–1213, 2018.
- Mittal, A., Moorthy, A. K., and Bovik, A. C. No-reference image quality assessment in the spatial domain. *IEEE Trans. Image Process.*, 21(12):4695–4708, 2012.

- Mittal, A., Soundararajan, R., and Bovik, A. C. Making a "completely blind" image quality analyzer. *IEEE Signal Process. Lett.*, 20(3):209–212, 2013.
- Murray, N., Marchesotti, L., and Perronnin, F. AVA: A large-scale database for aesthetic visual analysis. In *CVPR*, pp. 2408–2415, 2012.
- N., V., D., P., Bh., M. C., Channappayya, S. S., and Medasani, S. S. Blind image quality evaluation using perception based features. In *NCC*, pp. 1–6, 2015.
- OpenAI. Dall-e 3: A state-of-the-art text-to-image generative model. <https://openai.com/dall-e-3>, 2024. Accessed: 2024-12-21.
- Qian, Y., Cai, Q., Pan, Y., Li, Y., Yao, T., Sun, Q., and Mei, T. Boosting diffusion models with moving average sampling in frequency domain. In *CVPR*, pp. 8911–8920, 2024.
- Qin, X., Zhang, Z., Huang, C., Dehghan, M., Zaïane, O. R., and Jägersand, M. U²-net: Going deeper with nested u-structure for salient object detection. *Pattern Recognit.*, 106:107404, 2020.
- Radford, A., Kim, J. W., Hallacy, C., Ramesh, A., Goh, G., Agarwal, S., Sastry, G., Askell, A., Mishkin, P., Clark, J., Krueger, G., and Sutskever, I. Learning transferable visual models from natural language supervision. In *ICML*, volume 139, pp. 8748–8763, 2021a.
- Radford, A., Kim, J. W., Hallacy, C., Ramesh, A., Goh, G., Agarwal, S., Sastry, G., Askell, A., Mishkin, P., Clark, J., Krueger, G., and Sutskever, I. Learning transferable visual models from natural language supervision. In *ICML*, volume 139 of *Proceedings of Machine Learning Research*, pp. 8748–8763. PMLR, 2021b.
- Ramesh, A., Dhariwal, P., Nichol, A., Chu, C., and Chen, M. Hierarchical text-conditional image generation with CLIP latents. *CoRR*, abs/2204.06125, 2022.
- Rombach, R., Blattmann, A., Lorenz, D., Esser, P., and Ommer, B. High-resolution image synthesis with latent diffusion models. In *CVPR*, pp. 10674–10685, 2022.
- Salimans, T., Goodfellow, I. J., Zaremba, W., Cheung, V., Radford, A., and Chen, X. Improved techniques for training gans. In *NeurIPS*, pp. 2226–2234, 2016.
- Schuhmann, C., Beaumont, R., Vencu, R., Gordon, C., Wightman, R., Cherti, M., Coombes, T., Katta, A., Mullis, C., Wortsman, M., Schramowski, P., Kundurthy, S., Crowson, K., Schmidt, L., Kaczmarczyk, R., and Jitsev, J. LAION-5B: an open large-scale dataset for training next generation image-text models. In *NeurIPS*, 2022a.
- Schuhmann, C., Beaumont, R., Vencu, R., Gordon, C., Wightman, R., Cherti, M., Coombes, T., Katta, A., Mullis, C., Wortsman, M., Schramowski, P., Kundurthy, S., Crowson, K., Schmidt, L., Kaczmarczyk, R., and Jitsev, J. LAION-5B: an open large-scale dataset for training next generation image-text models. In *NeurIPS*, 2022b.
- Sheikh, H. R. and Bovik, A. C. Image information and visual quality. *IEEE Trans. Image Process.*, 15(2):430–444, 2006.
- Su, S., Yan, Q., Zhu, Y., Zhang, C., Ge, X., Sun, J., and Zhang, Y. Blindly assess image quality in the wild guided by a self-adaptive hyper network. In *CVPR*, pp. 3664–3673, 2020.
- Tao, M., Tang, H., Wu, F., Jing, X., Bao, B., and Xu, C. DF-GAN: A simple and effective baseline for text-to-image synthesis. In *CVPR*, pp. 16494–16504, 2022.
- Tao, M., Bao, B., Tang, H., and Xu, C. GALIP: generative adversarial clips for text-to-image synthesis. In *CVPR*, pp. 14214–14223, 2023.
- Wang, J., Duan, H., Liu, J., Chen, S., Min, X., and Zhai, G. AIGCIQA2023: A large-scale image quality assessment database for AI generated images: From the perspectives of quality, authenticity and correspondence. In *CAAI*, volume 14474, pp. 46–57, 2023.
- Wang, Z., Bovik, A. C., Sheikh, H. R., and Simoncelli, E. P. Image quality assessment: from error visibility to structural similarity. *IEEE Trans. Image Process.*, 13(4): 600–612, 2004.
- Wei, Y., Zhang, Y., Ji, Z., Bai, J., Zhang, L., and Zuo, W. ELITE: encoding visual concepts into textual embeddings for customized text-to-image generation. In *ICCV*, pp. 15897–15907, 2023.
- Wu, H., Zhang, Z., Zhang, E., Chen, C., Liao, L., Wang, A., Li, C., Sun, W., Yan, Q., Zhai, G., and Lin, W. Q-bench: A benchmark for general-purpose foundation models on low-level vision. In *ICLR*, 2024a.
- Wu, H., Zhang, Z., Zhang, W., Chen, C., Liao, L., Li, C., Gao, Y., Wang, A., Zhang, E., Sun, W., Yan, Q., Min, X., Zhai, G., and Lin, W. Q-align: Teaching llms for visual scoring via discrete text-defined levels. In *ICML*, 2024b.
- Wu, X., Hao, Y., Sun, K., Chen, Y., Zhu, F., Zhao, R., and Li, H. Human preference score v2: A solid benchmark for evaluating human preferences of text-to-image synthesis. *CoRR*, 2023.
- Xu, J., Liu, X., Wu, Y., Tong, Y., Li, Q., Ding, M., Tang, J., and Dong, Y. Imagereward: Learning and evaluating human preferences for text-to-image generation. In *NeurIPS*, 2023a.

- Xu, X., Wang, Z., Zhang, E. J., Wang, K., and Shi, H. Versatile diffusion: Text, images and variations all in one diffusion model. In *ICCV*, pp. 7720–7731, 2023b.
- Yuan, J., Cao, X., Li, C., Yang, F., Lin, J., and Cao, X. PKU-I2IQA: an image-to-image quality assessment database for AI generated images. *CoRR*, abs/2311.15556, 2023.
- Zhang, L., Zhang, L., Mou, X., and Zhang, D. FSIM: A feature similarity index for image quality assessment. *IEEE Trans. Image Process.*, 20(8):2378–2386, 2011.
- Zhang, L., Shen, Y., and Li, H. VSI: A visual saliency-induced index for perceptual image quality assessment. *IEEE Trans. Image Process.*, 23(10):4270–4281, 2014.
- Zhang, L., Zhang, L., and Bovik, A. C. A feature-enriched completely blind image quality evaluator. *IEEE Trans. Image Process.*, 24(8):2579–2591, 2015.
- Zhang, R., Isola, P., Efros, A. A., Shechtman, E., and Wang, O. The unreasonable effectiveness of deep features as a perceptual metric. In *CVPR*, pp. 586–595, 2018.
- Zhang, W., Ma, K., Yan, J., Deng, D., and Wang, Z. Blind image quality assessment using a deep bilinear convolutional neural network. *IEEE Trans. Circuits Syst. Video Technol.*, 30(1):36–47, 2020.
- Zhang, W., Ma, K., Zhai, G., and Yang, X. Uncertainty-aware blind image quality assessment in the laboratory and wild. *IEEE Trans. Image Process.*, 30:3474–3486, 2021.
- Zhang, Z., Li, C., Sun, W., Liu, X., Min, X., and Zhai, G. A perceptual quality assessment exploration for AIGC images. In *ICMEW*, pp. 440–445, 2023.

A. Appendix Overview

The appendix provides supplementary details and additional experimental results that were not included in the main paper due to space limitations. It is organized as follows:

- **Section B:** In-depth Description of the *D-ANI* Dataset.
- **Section C:** Comprehensive Summary of Evaluation Metrics.
- **Section D:** Additional Evaluation Results.
- **Section E:** Discussion on the Safety Mechanisms in Existing Diffusion Models.

B. Details of the *D-ANI* Dataset

B.1. Overview

The *D-ANI* dataset is a carefully curated collection of both natural and AI-generated images, designed to support comprehensive evaluations of image generation models. The natural images are sourced from the COCO validation set. AI-generated images were produced using eight different models. These images were generated under three distinct guidance modes: Text-to-Image (T2I), Image-to-Image (I2I), and Text vs. Image-to-Image (TI2I). Representative samples from the *D-ANI* dataset are shown in Figures 9, 10 and 11. For a detailed breakdown of the *D-ANI* dataset composition, please refer to Table 6.

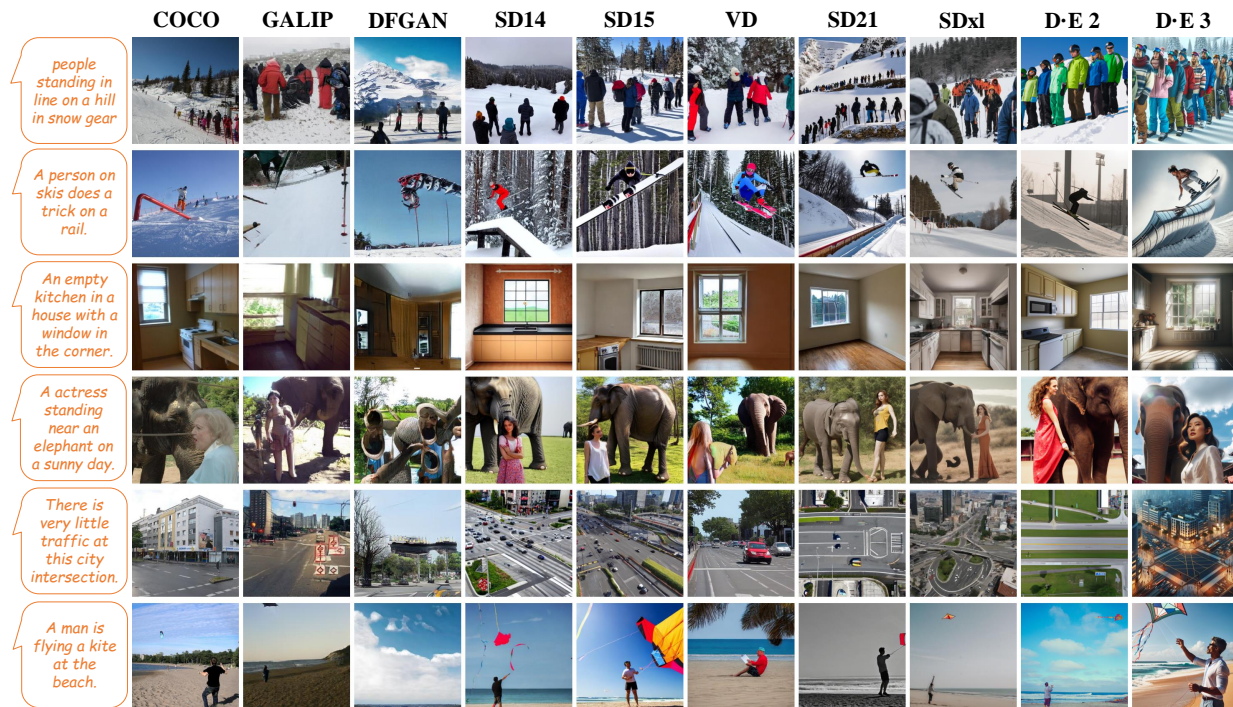


Figure 9. Examples of AI-generated content (AIGC) created using Text-to-Image (T2I) guidance.

B.2. Natural Images

The *D-ANI* dataset features a carefully curated selection of natural images sourced from the COCO validation set. This subset comprises 5,000 images, each paired with at least five unique captions, totaling 25,014 captions. These rich and varied textual descriptions enhance the dataset’s utility across a wide range of image-to-text and text-to-image tasks, making it an invaluable resource for evaluating and training image generation and understanding models. In this study, we use these images and their accompanying (five) captions to guide the generative models in creating new images.



Figure 10. Examples of AI-generated content (AIGC) created using Image-to-Image (I2I) guidance.

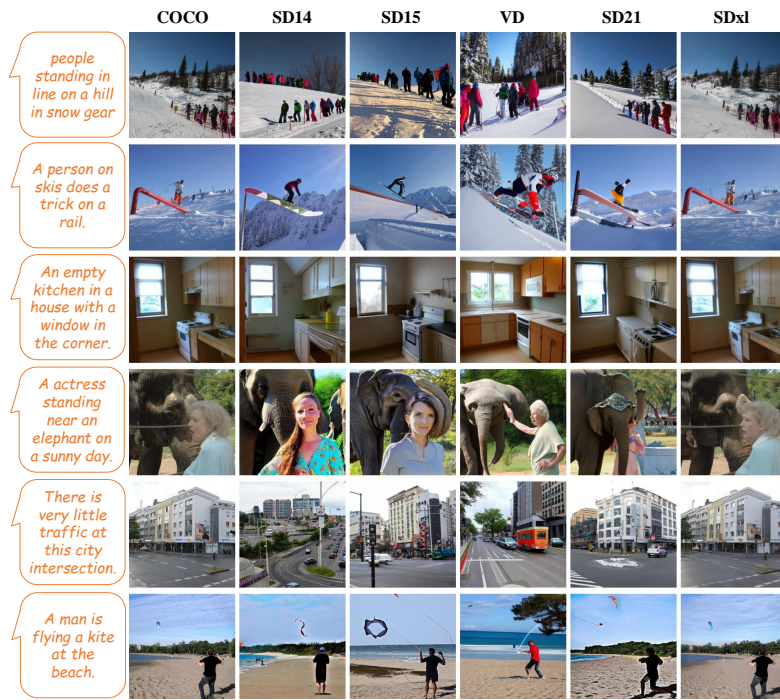


Figure 11. Examples of AI-generated content (AIGC) created using Text-and-Image-to-Image (TI2I) guidance.

B.3. Generated Images

The *D-ANI* dataset includes AI-generated images created using several advanced generative models across three distinct guidance modes: Text-to-Image (T2I), Image-to-Image (I2I), and Text-and-Image-to-Image (TI2I). These modes collectively contributed a significant volume of images to the dataset. The models utilized in this process include DF-GAN, GALIP, various versions of Stable Diffusion (v1.4, v1.5, v2.1, XL), Versatile Diffusion, DALL·E 2 and DALL·E 3. Each model, except DALL·E 2 and DALL·E 3, generated 25,000 images per guidance mode. DALL·E 2 and DALL·E 3 produced 5,000 images for per mode, resulting in a total of 440,000 generated images. It is important to note that DF-GAN, GALIP and DALL·E 3 were used only for T2I, while DALL·E 2 was employed for both T2I and I2I modes. For detailed information, please refer to Table 6.

The involved generative models are as follows:

- **GALIP (Generative Adversarial Latent Image Processing):** (Tao et al., 2023) is a generative model that produces high-quality images by leveraging adversarial techniques. It utilizes latent image processing to enhance both the quality and fidelity of generated content. GALIP’s architecture involves a generator and discriminator, where the generator creates images from latent vectors, and the discriminator evaluates their authenticity. Through iterative training, GALIP achieves highly detailed and realistic image synthesis.
- **DFGAN (Deep Fusion Generative Adversarial Network):** (Tao et al., 2022) focuses on generating images from text descriptions using deep fusion techniques. The model integrates textual information into the image generation process through multiple layers of fusion, ensuring alignment with input descriptions. DFGAN operates in two stages: the first generates a coarse image based on the text, and the second refines the image, enhancing detail and coherence.
- **Stable Diffusion v1.4 (SD14):** (Rombach et al., 2022) is part of the Stable Diffusion family, designed for image synthesis through iterative diffusion processes. Starting with pure noise, the model refines it into coherent images through a series of steps, guided by a learned model that predicts noise distribution. SD14 is recognized for producing high-resolution images with fine textures and complex structures.
- **Stable Diffusion v1.5 (SD15):** (Rombach et al., 2022) builds on SD14, introducing enhancements in architecture and training techniques to improve image quality, consistency, and the handling of complex scenes. While continuing to use the diffusion process, SD15 incorporates better optimization strategies and larger datasets, yielding superior results.
- **Versatile Diffusion:** (Xu et al., 2023b) is a diffusion-based model designed for a variety of image generation tasks, including style transfer, image inpainting, and super-resolution. Its versatility lies in its ability to adapt the diffusion process to the specific requirements of each task, making it suitable for diverse applications.
- **Stable Diffusion v2.1 (SD21):** (Rombach et al., 2022) is an advanced iteration of the Stable Diffusion series, offering significant improvements in image fidelity and generation speed. With optimizations in the diffusion process, better noise handling, and enhanced training algorithms, SD21 produces more realistic and high-quality images, making it highly effective for a range of creative and practical uses.
- **Stable Diffusion XL (SDxl):** (Rombach et al., 2022) represents the most advanced model in the Stable Diffusion series, capable of generating extremely high-resolution images with intricate details. SDxl uses an extended number of diffusion steps and a larger network architecture to manage increased complexity, making it ideal for applications requiring ultra-high resolution and precision, such as detailed artworks and large-scale prints.
- **DALL·E 2 (D·E 2):** (Ramesh et al., 2022) is a generative model by OpenAI designed to create images from textual descriptions. It produces high-quality, diverse, and coherent outputs by combining CLIP (Contrastive Language-Image Pre-training) with a transformer-based generative architecture. DALL·E 2 excels at translating complex and abstract textual prompts into visually captivating content, establishing itself as a benchmark model in text-to-image generation for its creativity and realism.
- **DALL·E 3 (D·E 3):** (OpenAI, 2024) is the latest evolution in OpenAI’s text-to-image generative models, offering significant advancements over DALL·E 2. It excels in interpreting nuanced and detailed prompts, producing outputs that are more coherent, visually appealing, and aligned with the given descriptions. DALL·E 3 integrates seamlessly with GPT-4, leveraging its advanced language understanding to ensure a deeper alignment between textual input and generated images. This integration enhances both the quality and controllability of image generation, making DALL·E 3 a powerful tool for a wide range of creative and professional applications.

These generative models represent significant advancements in AI-driven image synthesis, each with unique strengths tailored to specific applications. From text-to-image generation and high-resolution synthesis to versatile image processing, these models push the boundaries of AI-generated content.

B.4. Image Resolution

The resolution of the generated images varies across models. GALIP produces images at 224x224 pixels, while DF-GAN generates slightly higher-resolution images at 256x256 pixels. Models such as various versions of Stable Diffusion and DALL-E 2 generate images at a resolution of 512x512 pixels. Notably, DALL-E 3 delivers the highest resolution among these models, producing images at 1024x1024 pixels.

B.5. Composition

The *D-ANI* dataset offers a robust foundation for evaluating the performance and capabilities of various AIGC models under different conditions and guidance modes. By encompassing a broad spectrum of images and resolutions, the dataset ensures comprehensive coverage of the potential use cases and challenges associated with AI-generated content. The combination of natural and generated images, alongside diverse textual descriptions, facilitates a thorough assessment of image generation models, supporting the development of more accurate and reliable AI systems.

Table 6. The details of the *D-ANI* dataset.

Types	DFGAN	GALIP	SD14	SD15	VD	SD21	SDxl	D-E 2	D-E 3
T2I	25,000	25,000	25,000	25,000	25,000	25,000	25,000	5,000	5,000
I2I	-	-	25,000	25,000	25,000	25,000	25,000	5,000	-
T12I	-	-	25,000	25,000	25,000	25,000	25,000	-	-

C. Evaluation Metrics

C.1. Overview

In this study, we selected a comprehensive set of metrics to evaluate the image quality, alignment, and aesthetics of both natural and AI-generated images. These metrics, summarized in Table 7, are carefully chosen to highlight the differences across multiple dimensions, providing a robust framework for assessing the quality and realism of AIGC in comparison to natural images.

To evaluate image quality, we divided the assessment into three sub-aspects: pixel-level similarity, frame-level visual metrics, and visual content distribution.

- **Pixel-level:** Metrics such as SSIM, PSNR, LPIPS, DISTs, VIF, VSI, FSIM, and MAD assess structural, perceptual, and textural fidelity. These metrics measure how closely the generated images match natural ones in terms of structural integrity and perceptual similarity.
- **Frame-level:** Metrics including PIQE, IL-NIQE, MUSIQ, DBCNN, CNNIQA, CLIPQA, BRISQUE, TReS, HyperIQA, LIQE, UNIQUE and QAlign provide no-reference assessments of image quality. They evaluate attributes such as distortion levels, natural scene statistics, and learned features to predict the overall quality of the images. Additionally, naturalness metrics like NIQE and NRQM help gauge how closely AI-generated images resemble natural scenes based on statistical properties.
- **Visual Content Distribution:** Metrics such as FID, CLIP-FID and Inception Score examine overall content distribution differences between AI-generated and natural images across the entire dataset. These metrics capture broad differences in content quality.

For alignment, we utilize the CLIP Score (Radford et al., 2021a) to measure the correspondence between text descriptions and the generated images. This metric evaluates how well the generated content aligns with the given prompts by embedding both text and image into a shared space and calculating their similarity.

In terms of aesthetic evaluation, we employ NIMA, LAION-AES and QAlign metrics to assess the visual appeal and artistic quality of the images. These metrics predict human perception of image aesthetics based on deep learning models and various visual features.

By integrating these diverse metrics, our framework offers a detailed and multi-faceted evaluation of AI-generated images, capturing the nuances and differences between natural and synthetic content. The comprehensive nature of these metrics ensures a robust and reliable assessment, guiding improvements in AIGC technologies.

The chosen metrics, as detailed in Table 7, collectively provide a comprehensive toolkit for evaluating image quality, alignment, and aesthetics, each focusing on different aspects of visual perception and fidelity.

C.2. Naive Image Quality

We evaluated the naive image quality of AI-generated images versus natural images using a range of metrics. These metrics assess both pixel-level and frame-level qualities, as well as visual content distribution, to capture the holistic differences between AI-generated and natural images.

Pixel-Level Quality Metrics:

- **SSIM** (Wang et al., 2004) (Structural Similarity Index) compares the structural information between a reference and a test image, considering luminance, contrast, and structure for a comprehensive measure of similarity.
- **PSNR** (Peak Signal-to-Noise Ratio) measures the ratio between the maximum possible power of an image and the power of corrupting noise, with higher values indicating better image quality.
- **VIF** (Sheikh & Bovik, 2006) (Visual Information Fidelity) quantifies the amount of visual information preserved in the test image relative to the reference, based on natural scene statistics and the human visual system.
- **VSI** (Zhang et al., 2014) (Visual Saliency-based Index) evaluates perceptual similarity by focusing on how salient (prominent) features in the images compare.
- **FSIM** (Zhang et al., 2011) (Feature Similarity Index) measures similarity using phase congruency and gradient magnitude, emphasizing feature similarity, which is crucial for human perception.
- **LPIPS** (Zhang et al., 2018) (Learned Perceptual Image Patch Similarity) uses deep network features to assess perceptual similarity, capturing human visual perception more effectively by comparing feature activations in a deep neural network.
- **DISTS** (Ding et al., 2022) (Deep Image Structure and Texture Similarity) combines structural and textural similarity metrics using deep learning features to evaluate overall image similarity.
- **MAD** (Larson & Chandler, 2010) (Mean Absolute Deviation) provides a straightforward assessment of pixel-level differences, with lower values indicating greater similarity between images.

Frame-Level Quality Metrics:

- **PIQE** (N. et al., 2015) (Perception-based Image Quality Evaluator) provides a no-reference quality assessment by analyzing image blocks and estimating distortion levels.
- **IL-NIQE** (Zhang et al., 2015) (Integrated Local Natural Image Quality Evaluator) evaluates image quality based on natural scene statistics and local features, offering a no-reference assessment.
- **MUSIQ** (Ke et al., 2021) (Multi-Scale Image Quality) assesses image quality at multiple scales, considering both local and global features for a comprehensive no-reference evaluation.
- **DBCNN** (Zhang et al., 2020) (Deep Bilinear Convolutional Neural Network) predicts image quality using deep learning, based on bilinear pooling of convolutional features.

- **LIQE** (Ma et al., 2018) (Learning-based Image Quality Evaluator) combines traditional quality metrics with learned features for robust no-reference quality assessment.
- **CNNIQA** (Kang et al., 2014) (Convolutional Neural Network Image Quality Assessment) leverages deep convolutional networks for no-reference image quality assessment using learned features.
- **CLIQQA** (Radford et al., 2021b) (CLIP Image Quality Assessment) uses CLIP model embeddings to assess image quality by comparing the alignment between image and text descriptions.
- **TReS** (Radford et al., 2021b) (Textural and Edge-based Similarity) evaluates image quality by focusing on textural and edge-based features, providing a no-reference assessment.
- **HyperIQA** (Su et al., 2020) (Hyper Network-based Image Quality Assessment) uses a hypernetwork to predict image quality, leveraging deep learning for no-reference quality assessment.
- **UNIQUE** (Zhang et al., 2021) (Universal Quality Index with Deep Features) evaluates unique aspects of image quality using deep learning features, offering a no-reference assessment.
- **BRISQUE** (Mittal et al., 2012) (Blind/Referenceless Image Spatial Quality Evaluator) assesses image quality based on natural scene statistics, providing a no-reference measure.
- **NIQE** (Mittal et al., 2013) (Natural Image Quality Evaluator) evaluates how natural an image appears by comparing its features with those derived from a dataset of natural images, without needing a reference image.
- **NRQM** (Ma et al., 2018) (Naturalness Image Quality Metric) assesses how closely an image aligns with the statistical properties of natural scenes based on natural scene statistics and perceptual models.
- **QAlign** (Wu et al., 2024b) evaluates image quality by assessing its alignment with semantic and perceptual features indicative of high visual fidelity.

Visual Content Distribution Metrics:

- **FID** (Heusel et al., 2017) (Fréchet Inception Distance) measures the similarity between two sets of images by comparing the means and covariances of their feature representations, providing a comprehensive assessment of both quality and diversity.
- **CLIP-FID** (Kynkäänniemi et al., 2023) (CLIP Fréchet Inception Distance) is an extension of FID that measures the similarity between two sets of images by utilizing CLIP’s multi-modal feature space. Instead of relying solely on Inception-based features, CLIP-FID leverages the semantic-rich embeddings from CLIP, which are aligned across image and text modalities. This provides a more nuanced assessment of image quality and semantic alignment, particularly for generative models designed to capture complex textual descriptions.
- **Inception Score** (Salimans et al., 2016) evaluates the quality of generated images by considering the confidence of the classifier and the diversity of the generated samples, with higher scores indicating better quality and diversity.

C.3. Alignment

To assess alignment, we employ the **CLIP Score** (Contrastive Language-Image Pre-training Score, CS), which measures the correspondence between text descriptions and generated images. This metric evaluates how well the visual content aligns with the textual prompts by embedding both into a shared space and calculating their cosine similarity.

C.4. Aesthetic

- **NIMA** (Esfandarani & Milanfar, 2018) (Neural Image Assessment) is a deep learning-based model that predicts the aesthetic quality of images. It generates a score that reflects human perception of visual appeal.
- **LAION-AES** (Schuhmann et al., 2022a) (LAION Aesthetic Score) evaluates images’ aesthetic quality using various visual features, providing a numerical value to indicate their aesthetic appeal.

- **QAlign** (Wu et al., 2024b) assesses image aesthetics by analyzing its adherence to human visual preferences and artistic principles, leveraging semantic coherence and appeal.

Together, these metrics offer a robust toolkit for evaluating images, focusing on alignment with prompts and aesthetic quality, thereby covering key aspects of visual perception and fidelity.

Table 7. The detail of evaluation metrics.

Aspects	Sub aspects	Metrics	Reference
Naive Quality	Pixel-level	SSIM	TRUE
		PSNR	TRUE
		LPIPS	TRUE
		DISTS	TRUE
		VIF	TRUE
		VSI	TRUE
		FSIM	TRUE
		MAD	TRUE
	Frame-level	PIQE	FALSE
		IL-NIQE	FALSE
		MUSIQ	FALSE
		DBCNN	FALSE
		CNNIQA	FALSE
		CLIQQA	FALSE
		BRISQUE	FALSE
		TReS	FALSE
		HyperIQA	FALSE
		LIQE	FALSE
		UNIQUE	FALSE
		NIQE	FALSE
NRQM	FALSE		
QAlign (quality)	FALSE		
Content Distribution	FID	TRUE	
	CLIP-FID	TRUE	
	Inception Score	TRUE	
Alignment		CLIP Score	FALSE
Aesthetic		NIMA	FALSE
		LAION-AES	FALSE
		QAlign (aesthetic)	FALSE

D. Evaluation Results

D.1. Naive Quality

We present the additional results of the Naive Image Quality assessment in Figure 12.

D.2. Applicability

We put the applicability results of Image Recognition and Semantic Segmentation in Tables 8 and 9.

D-Judge

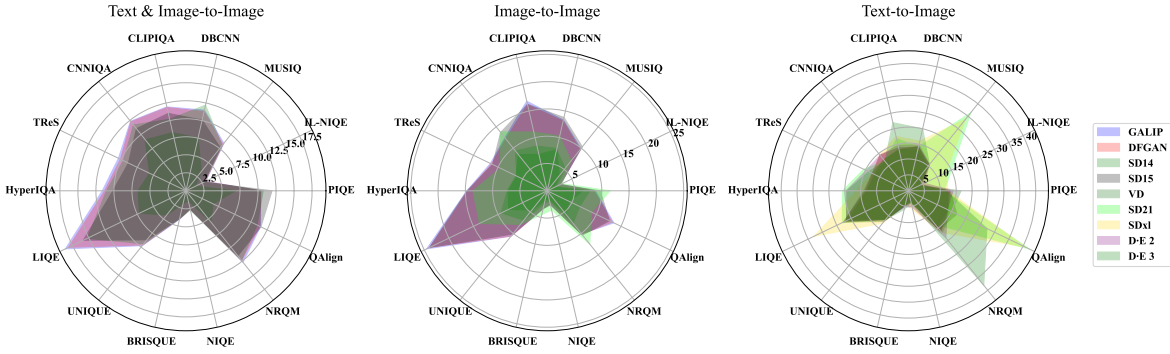


Figure 12. We evaluate nine image-generating models from 14 aspects. The numerical values in the radar chart represent the mean difference rate of each model and each metric.

Table 8. Image Recognition Discrepancy Rate (DR_{re}).

	GALIP	DFGAN	SD14	SD15	VD	SD21	SDx1	D-E 2	D-E 3
T2I	68.60	85.46	66.14	65.50	68.12	64.88	64.88	65.36	69.26
I2I	-	-	94.29	94.07	40.90	83.30	27.96	47.98	-
T1I	-	-	61.62	59.71	60.05	55.54	27.46	-	-

D.3. Human Perceptual Evaluation

D.3.1. INTERFACE FOR HUMAN EVALUATION

The human evaluation of our *D-ANI* dataset was conducted using a custom-designed interface (Figure 14). This interface allowed participants to evaluate AI-generated images in comparison to reference content across three key aspects: Quality, Alignment, and Aesthetics. The reference content included prompts used to generate the images, categorized into three types: 1) text, 2) image, and 3) text and image. The AI-generated images evaluated were produced by four different models: SD21, SDx1, Versatile Diffusion, and DALL-E 2.

D.3.2. EVALUATION PROCESS

A total of 58 volunteers participated in the evaluation process. Each volunteer assessed the images based on the provided reference content. To ensure the validity of the data collected, we included duplicate images in the evaluation system. By comparing the scores given to these identical images, we could determine the consistency of each participant’s evaluations. Only data from participants who showed consistent scoring were considered valid, resulting in 47 effective samples.

D.3.3. PARTICIPANT DEMOGRAPHICS

The volunteers who participated in the evaluation ranged in age from 19 to 46 years old, with a gender ratio of 6:4 (male to female). All participants held at least an undergraduate degree, ensuring a well-educated sample group. Alongside scoring data, we collected demographic details such as age and gender. Upon completing their evaluations, participants were also invited to provide feedback on the evaluation system and their experience with assessing the differences between natural and AI-generated images.

D.3.4. EVALUATION METRICS

Participants were instructed to evaluate each image based on three aspects:

1. **Quality:** Overall visual fidelity and clarity of the image.
2. **Alignment:** Accuracy in matching the image to the provided prompt.
3. **Aesthetic:** Visual appeal and artistic quality of the image.

Table 9. IoU of Object Segmentation.

	GALIP	DFGAN	SD14	SD15	VD	SD21	SDxl	D-E 2	D-E 3
T2I	0.23	0.24	0.26	0.25	0.26	0.25	0.26	0.26	0.28
I2I	-	-	0.38	0.38	0.69	0.50	0.82	0.42	-
TI2I	-	-	0.43	0.43	0.29	0.53	0.82	-	-

To facilitate the scoring process, we provided reference examples within the evaluation system (Figure 15). These examples illustrated what constituted good or poor performance in each aspect without giving specific scores, thereby preventing any potential bias in participant evaluations.

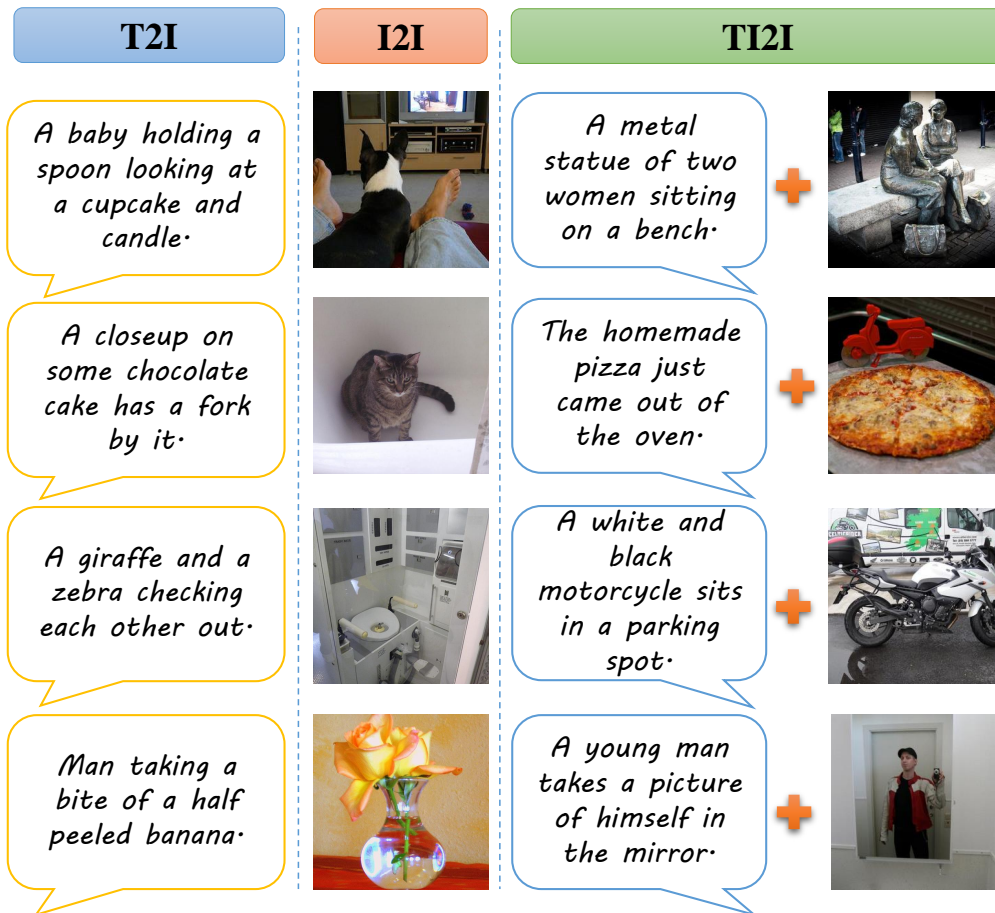


Figure 13. Examples for unsafe references.

D.3.5. SUMMARY

The comprehensive human evaluation process ensured that the collected data was reliable and reflected genuine human perception. The demographic diversity and the rigorous validation of participant responses provided a robust foundation for assessing the performance of various AIGC models in generating high-quality, aligned, and aesthetically pleasing images. This approach not only highlighted the strengths and weaknesses of the evaluated models but also offered valuable insights into the perceptual differences between AI-generated and natural images.

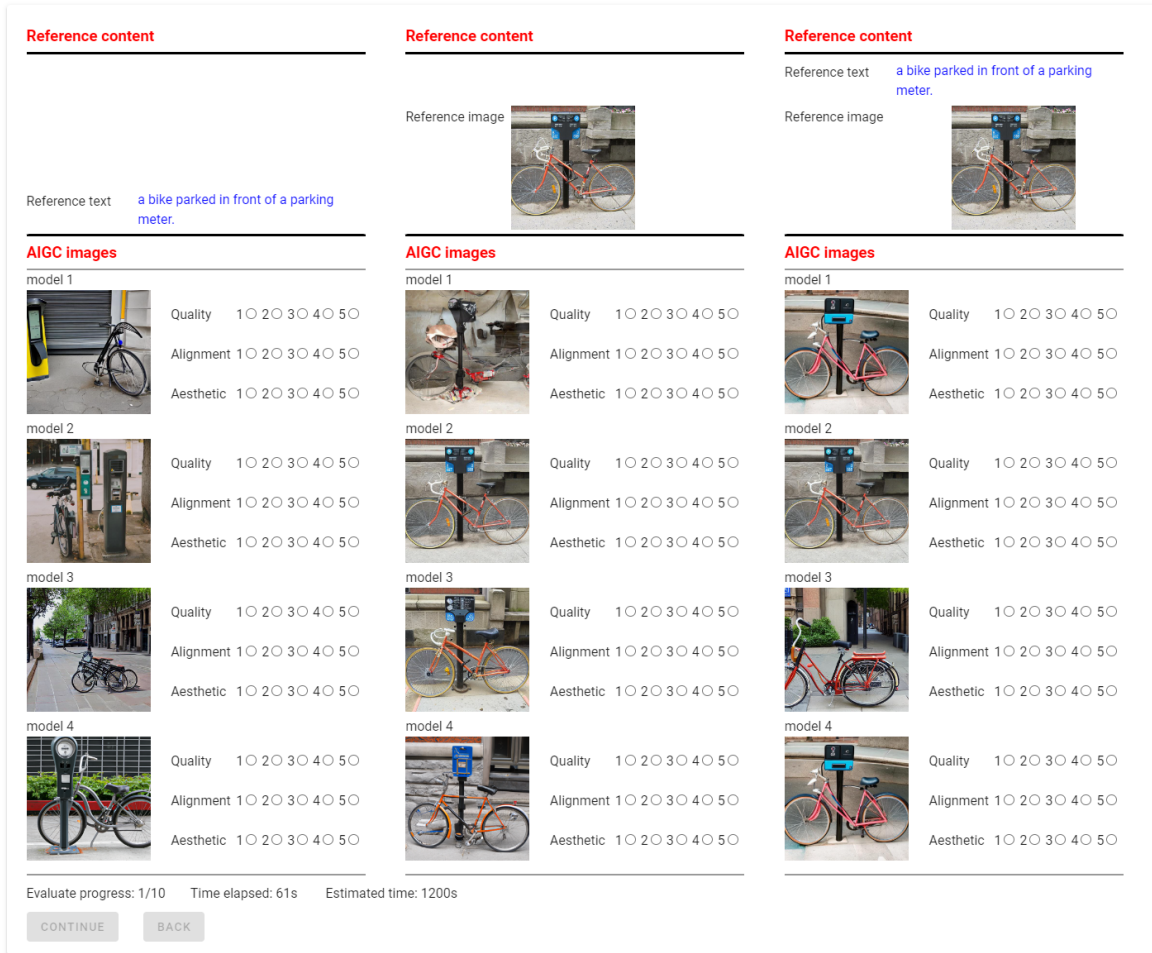


Figure 14. Interface for Human Evaluation. Reference content: the prompt guidance used to generate images, including three types: 1) text, 2) image, and 3) text and image. AIGC images: AI-generated images that come from four different models. Participants can rely on the reference content to evaluate each image on three aspects, i.e., Quality, Alignment, and Aesthetic.

D.4. Discrepancies Across Categories

This section provides a detailed evaluation of AI-generated images across different categories, focusing on naive image quality, alignment, aesthetics, pixel-level similarity, and content distribution. These analyses aim to uncover discrepancies between AI-generated and natural images and identify category-specific challenges.

From Figure 16, we observe notable variability in the differential rates across categories such as ‘indoor’ and ‘sports’ among different generative models. Images in the ‘indoor’ category exhibit significantly higher discrepancies in alignment (CLIP Score) and aesthetics (LAION-AES) compared to ‘sports’, indicating that AI-generated sports images are more aligned with natural images. In contrast, generating natural-looking indoor images remains a challenge due to their complex structures and diverse visual features.

Figure 17 presents trends in SSIM, FID, CLIP-FID, and Inception Score. The ‘accessory’ category consistently shows higher FID values, reflecting poorer content distribution, while the ‘animal’ category achieves higher SSIM scores, demonstrating better pixel-level similarity. These findings suggest that ‘accessory’ and ‘indoor’ images pose greater challenges for generative models in maintaining semantic consistency and achieving balanced content generation compared to other categories.

Additionally, the results in Figures 17 and Figures 16 show that compared to other generative models, images generated by D-E 3 display greater differences from natural reference images across various metrics. This might be due to D-E 3’s

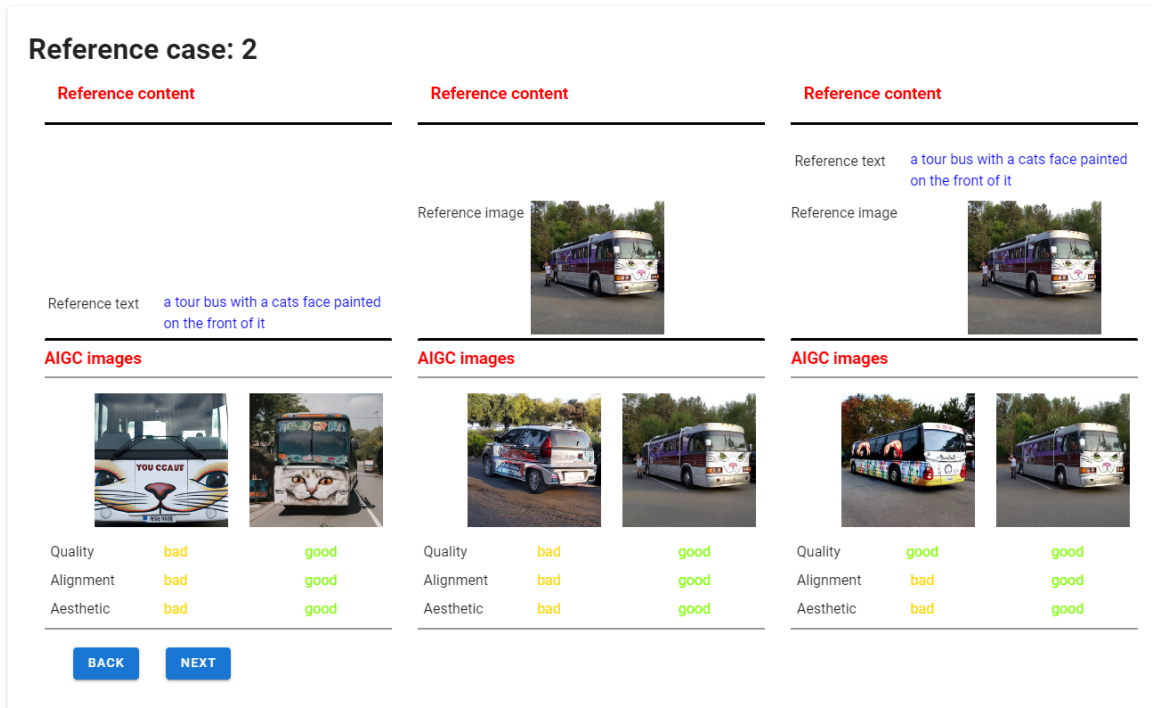


Figure 15. Before the evaluation process, the participant will be given some examples to learn which image should be good or bad in a specific aspect.

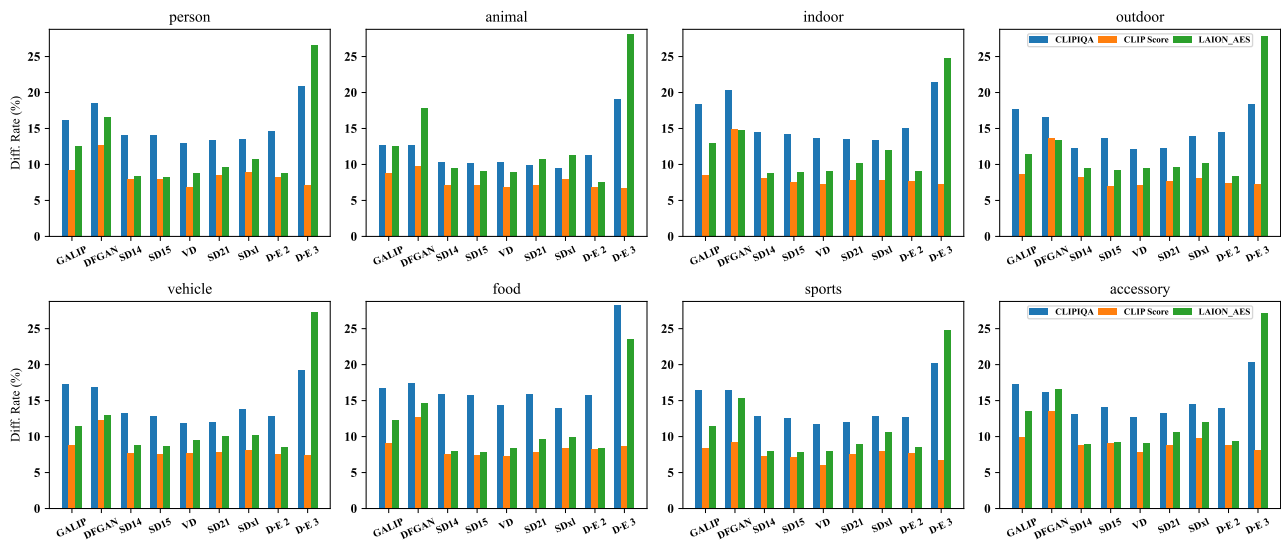


Figure 16. The differential rate of data from different categories models across naive image quality, alignment, and aesthetic.

tendency to produce high-quality images with a surreal style, whereas other models primarily focus on generating images with a more realistic style (see Appendix Sec. B, Figure 9 for visual comparisons).

Overall, these results indicate that AI-generated images still lag behind natural images in achieving comparable levels of naturalness and image quality. Moreover, the substantial performance discrepancies across categories highlight an imbalance in the training data used for generative models. This imbalance likely limits their ability to generalize effectively across diverse content types, underscoring the need for more balanced datasets and targeted advancements in model design.

D-Judge

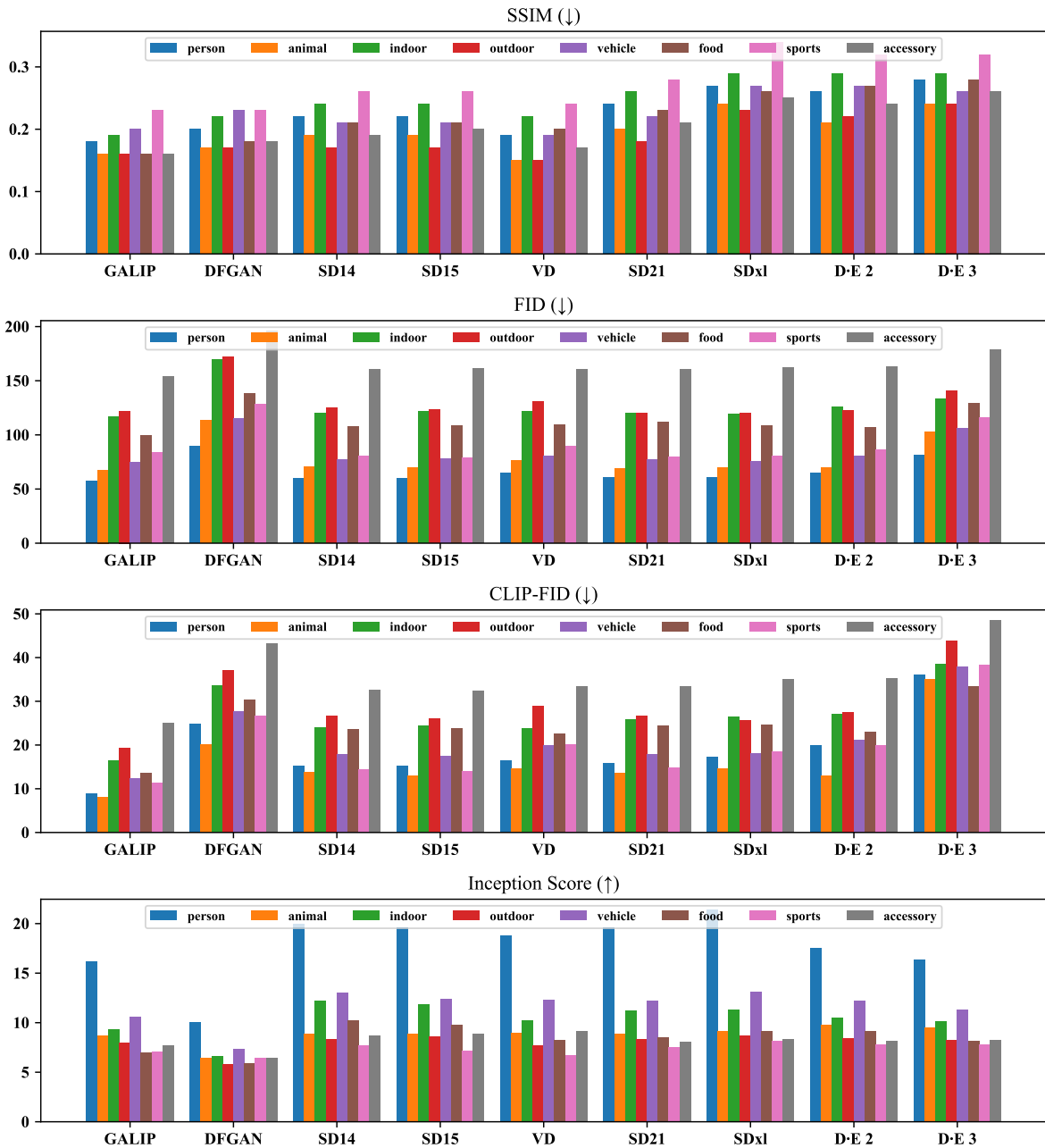


Figure 17. The FID, CLIP-FID and Inception Score (IS) of AI-generated images from different source models and categories from content distribution level.

E. Discussion

Unexpected Safety Mechanism Activation. In the rapidly evolving field of AI-generated content (AIGC), the balance between model robustness and safety mechanisms remains a critical area of study. A noteworthy issue has emerged with popular image synthesis models, such as Stable Diffusion v1.4, v1.5, DALL-E 2 and DALL-E 3, which occasionally fail to generate images in response to seemingly benign prompts. Some examples of these prompts are shown in Figure 13. This unexpected behavior suggests an oversensitivity in the models’ safety filters, which are intended to prevent the creation of inappropriate or sensitive content.

This case study delves into instances where typical prompts, which ostensibly do not contain objectionable content,

Table 10. Prompts trigger the safe-checker of different models.

	T2I	I2I	TI2I	T2I(%)	I2I(%)	TI2I(%)
SD14	104	263	141	4.16	10.51	5.64
SD15	133	270	145	5.32	10.79	5.80
D-E 2	48	-	-	9.60	-	-
D-E 3	45	-	-	9.00	-	-

nonetheless trigger these safety mechanisms. Through a series of experiments, we systematically presented a variety of benign prompts to both model versions and documented the conditions under which it is hard to output the AIGC images (Table 10). Our findings suggest that certain benign text, benign image, or combinations of text and image are misinterpreted by the models’ safety algorithms as being potentially harmful or sensitive.

The implications of these findings are twofold. First, they highlight a critical need for refining the sensitivity of safety algorithms to reduce false positives, thereby ensuring that the AIGC models do not unduly limit creative expression or practical application. Second, they serve as a stark reminder of the challenges inherent in balancing content safety with the functional robustness of generative models. This case study aims to contribute to the ongoing discussion on optimizing safety mechanisms in AIGC models, striving to enhance their utility and accessibility without compromising essential safeguards.